Inorg. Chem. **2005**, *44*, 875–883

N_2S_2Ni Metallodithiolate Complexes as Ligands: Structural and Aqueous Solution Quantitative Studies of the Ability of Metal Ions to Form M–S–Ni Bridges to Mercapto Groups Coordinated to Nickel(II). Implications for Acetyl Coenzyme A Synthase

Melissa L. Golden,[†] Curtis M. Whaley,[‡] Marilyn V. Rampersad,[†] Joseph H. Reibenspies,[†] Robert D. Hancock,*[,‡] and Marcetta Y. Darensbourg*[,†]

Departments of Chemistry, Texas A&M University, College Station, Texas 77843, and University of North Carolina at Wilmington, Wilmington, North Carolina 28403

Received July 30, 2004

The nickel(II) complex of an N_2S_2 ligand, derived from a diazacycle, *N*,*N*′-bis(mercaptoethyl)-1,5-diazacycloheptane, (bme-dach)Ni, **Ni-1′**, serves as a metallodithiolate ligand to Ni^{II}, Cu^{I}, Zn^{II}, Ag^{I}, and Pb^{II}. The binding ability of the NiN_2S_2 ligand to the metal ions was established through spectrochemical titrations in aqueous media and compared to classical S-donor ligands. For M = Ni, Zn, Pb, binding constants, log *K* = ca. 2, were computed for 1:1 **Ni-1′**/M(solvate) adducts; for Ag^+ and Cu^+, the 3:2 (**Ni-1′**)$_3M_2$ adducts were the first formed products even in water with log $\beta_{3,2}$ values of 26 and >30, respectively. In all cases, the binding ability of Ni–S–R is intermediate between that of a free thiolate and a free thioether. The great specificity for copper over nickel and zinc by N_2S_2Ni, which serves as a reasonable structural model for the distal nickel of the acetyl CoA synthase active site, relates to biochemical studies of heterogeneity (metal content and type) in various preparations of acetyl CoA synthase enzyme.

The coordination chemistry of mercapto groups, derived from cysteine residues on proteins, is of major importance in biology. A dominant theme in complexes of ligands having mercapto groups is the formation of bridges between metal ions by mercapto sulfurs, as shown by the coordination chemistry of a widely investigated simple ligand such as mercaptoethanol (ME). Thus, of the 28 structures of complexes of this ligand reported in the Cambridge Structural Database, the majority involve sulfur donors bridging between two metal ions; also, where there is no bridging, steric hindrance prevents it, or the coordination number of the complexed metal ion is already satisfied by the coordinated ligands present. Formation constant studies in solution show that for virtually all of the complexes of ME with metal ions studied, polymeric species are present in solution.[1] As an example, for Zn(II) with ME the postulated solution species include $[Zn_5(ME)_{12}]^{2-}$ and $[Zn_6(ME)_{15}]^{3-}$.[1]

Depicted below are nickel(II) complexes of N_2S_2 ligands derived from open chains such as *N*,*N*′-dimethyl-3,7-diazanonane-1,9-dithiolate (R = Me) or *N*,*N*′-dimethyl-3,7-diazanonane-1,9-dithiolate (R = Et), **A**;[2,3] *N*,*N*′-ethylenebis(2-mercaptoacetamide), **B**;[4] *N*,*N*′-bis(mercaptoethyl)-1,5-diazacyclooctane, the (bme-daco)Ni complex **C**;[5] and *N*,*N*′-bis(mercaptoethyl)-1,5-diazacycloheptane, (bme-dach)Ni, **D**.[6] Such complexes present cis dithiolates whose S-based reactivity with a wide range of electrophiles is well established. The complexes (bme-daco)Ni and (bme-dach)Ni are prospects for study of binding to a variety of metal ions where the discrete N_2S_2Ni complexes can act as S-donor ligands. The square planar Ni(II) within the N_2S_2 coordination sphere is coordinatively saturated, and so has no tendency to form Ni−S−Ni sulfide bridges with itself. However, the coordinated mercapto groups on such com-

* To whom correspondence should be addressed. E-mail: hancockr@uncw.edu (R.D.H.); marcetta@mail.chem.tamu.edu (M.Y.D.).
[†] Texas A&M University.
[‡] University of North Carolina at Wilmington.

(1) Martell, A. E.; Smith, R. M. *Critical Stability Constant Database, 46*; National Institute of Science and Technology (NIST): Gaithersburg, MD, 2003.
(2) Lippard, S. J. *Acc. Chem. Res.* **1973**, *6*, 282−288.
(3) Osterlohl, F.; Saak, W.; Pohl, S. *J. Am. Chem. Soc.* **1997**, *119*, 5648−5656.
(4) Krüger, H. J.; Peng, G.; Holm, R. H. *Inorg. Chem.* **1991**, *30*, 734−742.
(5) Mills, D. K.; Reibenspies, J. H.; Darensbourg, M. Y. *Inorg. Chem.* **1990**, *29*, 4364−4365.
(6) Smee, J. J.; Miller, M. L.; Grapperhaus, C. A.; Reibenspies, J. H.; Darensbourg, M. Y. *Inorg. Chem.* **2001**, *40*, 3601−3605.

10.1021/ic0489701 CCC: $30.25
Published on Web 01/05/2005

plexes may be shared with other metal ions, including some of biological importance, providing a unique opportunity to determine the relative binding abilities of a series of metal ions with a constant binding site consisting of a square planar Ni(II) with two sulfurs, which can form Ni−S−M bridges to the metal ion M.

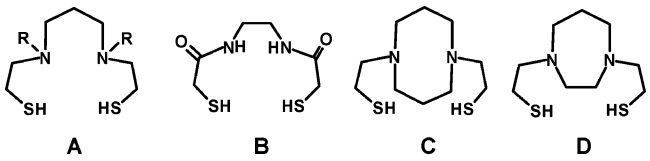

It has recently become apparent that such complexes serve as structural mimics of a biological N_2S_2Ni complex. As presented in Figure 1, structure **E**, the distal nickel, Ni_d, of the A-cluster in acetyl CoA synthase is in square planar coordination and comprises half of the active site.[7,8] This nickel(II) ion is chelated by two carboxamido nitrogen and two cysteinyl sulfurs of a Cys-Gly-Cys peptide sequence while a second nickel is attached to the same cysteines in μ-S_{Cys} binding. The coordination sphere of the second nickel (Ni_p, proximal to the iron−sulfur cluster) is completed by a nonproteinacious ligand L, assumed to be CH_3 or CO, and yet another μ-S_{Cys} which links the two-nickel site to a 4Fe4S cluster.[7,8] The simplicity of the binuclear component, coupled with the well-known, extensive literature of N_2S_2Ni complexes, rapidly led to homologous structural models including the Cys-Gly-Cys tripeptide Ni^{II}/Ni^{II} complex **F** of Riordan et al.,[9] and the model dicarboxamido dithiolate Ni^{II}/Ni^{0} complex **G** of Rauchfuss et al., Figure 1.[10] A copper analogue, **H**, of the latter demonstrated the feasibility of both Cu^{I} and Ni^{0} binding by the N_2S_2Ni metallothiolate ligand.[10] The sterically encumbered $P(^{i}Pr)_3$ ligand prevented the formation of aggregates such as the $(N_2S_2Ni)_3(CuBr)_2$ pinwheel structures observed by us.[11]

The importance of the NiCu heterobimetallic complex H derives from the first published protein crystal structure which found such a composition in the A cluster "active" site.[8] An initial controversy centered on which metal in the proximal site, Ni or Cu, conferred the biocatalytic function of ACS, i.e., the assembly of Me^{+}, CO, and SR^{-} to make MeC(═O)SR.[12−15] Consensus from subsequent biochemical

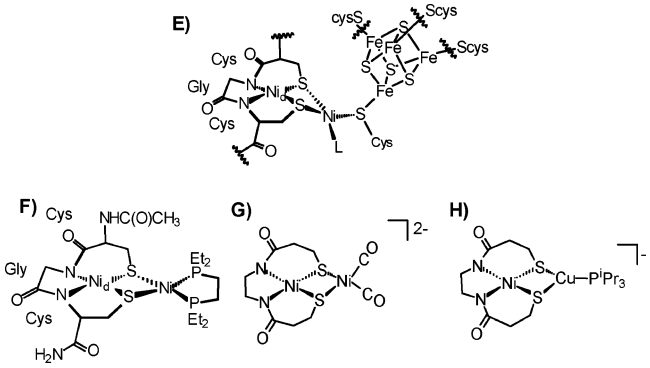

Figure 1. Representation of the active site in the α subunit of the ACS enzyme, **E**,[7,8] and three synthetic analogues, **F**,[9] **G**,[10] and **H**.[10]

and theoretical studies is that enzyme activity requires a NiNi formulation of the A cluster.[14,16−18]

The presence of other metals, copper and zinc, in the proximal metal site in some preparations of the ACS enzyme was consistent with a long known and vexing problem of heterogeneity and partial nickel lability, extensively explored for the bifunctional *Clostridium thermoaceticum* CODH/ACS enzyme and well-articulated by Lindahl et al.[19] That the N_2S_2Ni complex, (bme-daco)Ni, a reasonable structural model for the distal nickel of the ACS active site, showed a profound preference for binding copper(I) over nickel(II) or zinc(II) was qualitatively illustrated by the chemical reaction model studies of Golden et al.[11] In biochemical studies, Lindahl et al.[14] and subsequently Ragsdale et al.[17] similarly found that the ACS site, depleted in labile nickel, i.e., the proximal nickel, could take up copper from the protein expression medium from which the enzyme was isolated and compromise both the site integrity and enzyme function. Additional studies concluded that homometallic, i.e., dinickel, forms were solely responsible for significant catalytic activity in the active site of the enzyme;[12,14] that these nickels are in distinctly different sites was corroborated by X-ray spectroscopy results.[16]

While the transition metal ion requirements for ACS active site structure and function are now assured, unknowns remain regarding the mechanism of site assembly and the point at which the nickel-specific delivery process broke down and the copper-compromised active site developed in the isolated protein crystals which were used in the X-ray diffraction studies. Thus, research into the binding of exogenous metals by N_2S_2Ni has been stimulated.[9−11,20−22] In this context, the following study established binding affinities, including binding constants of Cu^{+} and Ag^{+} to the N_2S_2Ni complex,

(7) Darnault, C.; Volbeda, A.; Kim, E. J.; Legrand, P.; Vernède, X.; Lindahl, P. A.; Fontecilla-Camps, J. C. *Nat. Struct. Biol.* **2003**, *10*, 271−279.
(8) Doukov, T. I.; Iverson, T. M.; Seravalli, J.; Ragsdale, S. W.; Drennan, C. L. *Science* **2002**, *298*, 567−572.
(9) Krishnan, R.; Riordan, C. G. *J. Am. Chem. Soc.* **2004**, *126*, 4484−4485.
(10) Linck, R. C.; Spahn, C. W.; Rauchfuss, T. B.; Wilson, S. R. *J. Am. Chem. Soc.* **2003**, *125*, 8700−8701.
(11) Golden, M. L.; Rampersad, M. V.; Reibenspies, J. H.; Darensbourg, M. Y. *Chem. Commun.* **2003**, 1824−1825.
(12) Gencic, S.; Grahame, D. A. *J. Biol. Chem.* **2003**, *278*, 6101−6110.
(13) Seravalli, J.; Gu, W.; Tam, A.; Strauss, E.; Begley, T.; Cramer, S.; Ragsdale, S. *Proc. Natl. Acad. Sci. U.S.A.* **2003**, *100*, 3689−3694.
(14) Bramlett, M. R.; Tan, X.; Lindahl, P. A. *J. Am. Chem. Soc.* **2003**, *125*, 9316−9317.
(15) Wang, Q.; Blake, A. J.; Davies, E. S.; McInnes, E. J. L.; Wilson, C.; Schröder, M. *Chem. Commun.* **2003**, 3012−3013.
(16) Funk, T.; Gu, W.; Friedrich, S.; Wang, H.; Gencic, S.; Grahame, D. A.; Cramer, S. P. *J. Am. Chem. Soc.* **2004**, *126*, 88−95.
(17) Seravalli, J.; Xiao, Y.; Gu, W.; Cramer, S. P.; Antholine, W. E.; Krymov, V.; Gerfen, G. J.; Ragsdale, S. W. *Biochemistry* **2004**, *43*, 3944−3955.
(18) Webster, C. E.; Darensbourg, M. Y.; Lindahl, P. A.; Hall, M. B. *J. Am. Chem. Soc.* **2004**, *126*, 3410−3411.
(19) Lindahl, P. A. *Biochemistry* **2002**, *41*, 2097−2105.
(20) Hatlevik, Ø.; Blanksma, M. C.; Mathrubootham, V.; Arif, A. M.; Hegg, E. L. *J. Biol. Inorg. Chem.* **2004**, *9*, 238−246.
(21) Golden, M. L.; Jeffery, S.; Reibenspies, J. H.; Darensbourg, M. Y. *Eur. J. Inorg. Chem.* **2004**, 231−236.
(22) Miller, M. L.; Ibrahim, S. A.; Golden, M. L.; Darensbourg, M. Y. *Inorg. Chem.* **2003**, *42*, 2999−3007.

(bme-dach)Ni, in aqueous media, with semiquantitative comparisons to the weaker binding abilities of Ni^{2+}, Pb^{2+}, and Zn^{2+}.

Experimental Section

General Methods and Materials. While the compounds are not exceedingly air sensitive, all syntheses and manipulations of materials were carried out under an argon atmosphere using Schlenk techniques or a glovebox. Solvents were dried under a dinitrogen atmosphere prior to use according to published procedures.[23] The salts, $ZnCl_2$, $Zn(ClO_4)_2 \cdot 6H_2O$, CuBr, $AgClO_4$, $Pb(ClO_4)_2 \cdot 3H_2O$ (Aldrich Chemical Co.), $[Cu(NCMe)_4]PF_6$ (Strem), and $NiCl_2 \cdot 6H_2O$ (J. T. Baker), were used as received. *Caution!!!* Although no problems were encountered in this study, perchlorate salts are potentially explosive. Small quantities (<100 mg) are advised.

Physical Measurements. UV−vis spectra were recorded on a Hewlett-Packard HP8452A diode array spectrophotometer and a Cary1E spectrophotometer. Elemental analyses were performed by Canadian Microanalytical Systems in Delta, British Columbia, Canada. Mass spectral analyses were done at the Laboratory for Biological Mass Spectroscopy at Texas A&M University. Electrospray ionization mass spectra were recorded on water, acetonitrile, or MeOH/H_2O solutions using an MDS-Series QStar Pulsar with a spray voltage of 5 keV.

Syntheses. The dithiol (H_2-bme-dach), its nickel complex (**Ni-1′**), and $[(\mathbf{Ni\text{-}1'})_2Ni](Br)_2$ were synthesized according to published methods.[6] All preparations and isolations were carried out under an inert atmosphere of Ar or N_2 unless otherwise stated.

Preparation of $[(\mathbf{Ni\text{-}1'})_3Pb](ClO_4)_2$. Under an inert atmosphere, 30 mL of CH_3CN was added to **Ni-1′** (200 mg, 0.720 mmol). To this magnetically stirred tan slurry, a 30 mL CH_3CN solution of colorless $Pb(ClO_4)_2 \cdot 3H_2O$ (112 mg, 0.243 mmol) was added to yield a clear orange-red solution. The solution was stirred vigorously for 30 min. Solvent was then removed in vacuo, and the product was washed with ether. Crude yield: 286 mg, 96.0%. Hexane layering over an CH_3CN solution produced crystals of X-ray quality. UV−vis (acetonitrile), nm ($M^{-1}\,cm^{-1}$): 220 (36 700), 260 (44 500), 352 (7500). Elemental Anal. Calcd (Found) for $Ni_3PbC_{27}H_{54}N_6S_6Cl_2O_8$: C, 26.2 (26.1); N, 6.79 (6.71); H, 4.40 (4.33). Mass spectrum (CH_3CN solution) *m*/*z* (% abundance relative to base peak = 100%): 519 $\{(\mathbf{Ni\text{-}1'})_3Pb\}^{2+}$ (100%); 1137 $\{(\mathbf{Ni\text{-}1'})_3Pb(ClO_4)\}^{+}$ (1%); 380 $\{(\mathbf{Ni\text{-}1'})_2Pb\}^{2+}$ (70%); 861 $\{(\mathbf{Ni\text{-}1'})_2Pb(ClO_4)\}^{+}$ (3%).

Preparation of $[(\mathbf{Ni\text{-}1'})_3Cu_2Br](Br)$. To a deep tan slurry of **Ni-1′** (101 mg, 0.364 mmol in 50 mL of CH_3CN) was added a pale green CH_3CN solution of CuBr (34.8 mg, 0.243 mmol) dropwise resulting in an orange-brown solution. The solution was magnetically stirred vigorously for several hours, and the solvent was removed in vacuo. The resultant orange-brown solid was washed with ether. Crude yield: 78.6 mg, 58.0%. Purification by layering hexanes onto a CH_2Cl_2 solution of the product produced crystals of X-ray quality. UV−vis (acetonitrile), nm ($M^{-1}cm^{-1}$): 218 (32 700), 246 (25 300), 390 (1850), 440 (1550). Elemental Anal. Calcd (Found) for $Ni_3Cu_2C_{27}H_{54}N_6S_6Br_2 \cdot CH_2Cl_2$: C, 28.0 (27.8); N, 6.99 (6.73); H, 4.69 (4.93). (N.B. The crystal structure of this compound finds CH_2Cl_2 solvate molecules.) Mass spectrum (CH_3OH solution) *m*/*z* (% abundance): 478 $\{(\mathbf{Ni\text{-}1'})_3Cu_2\}^{2+}$ (100%); 617 $\{(\mathbf{Ni\text{-}1'})_3Cu\}^{+}$ (75%); 339 $\{(\mathbf{Ni\text{-}1'})Cu\}^{+}$ (95%); 1037 $\{(\mathbf{Ni\text{-}1'})_3Cu_2Br\}^{+}$ (5%).

Preparation of $[(\mathbf{Ni\text{-}1'})_3Ag_2](ClO_4)_2$. Methanol, 90 mL, was added to **Ni-1′** (200 mg, 0.720 mmol) producing a deep tan slurry to which a solution of $AgClO_4$ (95 mg, 0.457 mmol) dissolved in 30 mL CH_3OH was added. The peach-brown solution was stirred vigorously for 24 h. Solvent was then removed in vacuo, and the product was washed with ether. Crude yield: 250 mg, 88%. Purification by layering diethyl ether onto an CH_3CN solution of the product yielded crystals of X-ray quality. UV−vis (acetonitrile), nm ($M^{-1}\,cm^{-1}$): 214 (27 800), 242 (30 100), 264 (26 600), 360 (2000), 444 (730). Elemental Anal. Calcd (Found) for $Ni_3Ag_2C_{27}H_{54}N_6S_6Cl_2O_8$: C, 26.0 (25.8); N, 6.75 (7.12); H, 4.37 (4.40). Mass spectrum (CH_3CN solution) *m*/*z* (% abundance): 533 $\{(\mathbf{Ni\text{-}1'})_3Ag_2\}^{2+}$ (40%); 385 $\{(\mathbf{Ni\text{-}1'})\,Ag\}^{+}$ (100%); 661 $\{(\mathbf{Ni\text{-}1'})_2Ag\}^{+}$ (53%).

Preparation of $[(\mathbf{Ni\text{-}1'})_3(ZnCl)_2](Cl)_2$. A 30 mL MeOH solution of $ZnCl_2$ (76 mg, 0.558 mmol) was transferred to a 40 mL slurry of **Ni-1′** (206 mg, 0.742 mmol) in MeOH to make a red-orange solution. The product precipitated on addition of ether. Crude yield: 210 mg, 76.9%. To obtain crystals of X-ray quality an ion exchange was necessary. A methanol solution of $[(\mathbf{Ni\text{-}1'})_3(ZnCl)_2](Cl_2)$ was layered with a THF solution of $NaBF_4$ to yield red-orange crystals. UV−vis (acetonitrile), nm ($M^{-1}\,cm^{-1}$): 226 (34 000), 270 (27 200), 460 (530). Elemental Anal. Calcd (Found) for $Ni_3Zn_2C_{27}H_{54}N_6S_6Cl_2B_2F_8$: C, 26.9 (27.1); N, 6.97 (6.59); H, 4.51 (4.57). Mass spectrum, CH_3CN/CH_2Cl_2, *m*/*z* (% abundance): 377 $\{(\mathbf{Ni\text{-}1'})\,ZnCl\}^{+}$ (100%); 655 $\{(\mathbf{Ni\text{-}1'})_2ZnCl\}^{+}$ (54%).

Determination of Formation Constants. In a typical experiment, 25 mL of a 1.0×10^{-5} M solution of **Ni-1′** was placed in an external jacketed thermostated titration cell at 25.0 ± 0.1 °C. The solution in this external cell was circulated through a flow cell in the UV−vis spectrophotometer by means of a peristaltic pump. The external cell was titrated with 20−100 μL aliquots of a 0.1 M solution of the metal ion as its perchlorate salt (with the exception of $[Cu(NCCH_3)_4](PF_6)$). The concentrations of species were evaluated by plotting absorbance at selected wavelengths versus the ratio of ligand, **Ni-1′**, to metal, see Figure S1. While a simple 1:1 complex model (**Ni-1′**:M^+) was appropriate for Pb(II), Ni(II), and Zn(II), such simple models could not be fitted to the variations in peak intensity that were produced as a function of Cu(I) and Ag(I) metal ion concentration. A computer program was written that allowed various models of the type $[M_n(\mathbf{Ni\text{-}1'})_m]$ to be fitted to the data. As discussed below, for Cu(I) and Ag(I), good fits were obtained with $n = 2$ and $m = 3$; for Pb(II), Ni(II), and Zn(II), $n = m = 1$.

X-ray Crystal Structure Determinations. Low temperature, 110 K, X-ray diffraction data were collected on a Bruker SMART CCD-based diffractometer (Mo Kα radiation, $\lambda = 0.71073$ Å) and covered a hemisphere of space upon combining three sets of exposures. Empirical absorption corrections were applied with SADABS.[24] The space groups were determined on the basis of systematic absences and intensity statistics using the SMART[25] program for data collection and cell refinement. Raw data frame integration was performed with SAINT+.[26] Other programs used include SHELXS-86 (Sheldrick)[27] for structure solution, SHELXL-97 (Sheldrick)[28]

(23) Gordon, A. J.; Ford, R. A. *The Chemist's Companion*; Wiley and Sons: New York, 1972; pp 430−437.

(24) Sheldrick, G. *SHELXL-97: Program for Systematic Error Correction*; Institüt für Anorganische Chemie der Universität: Göttingen, Germany, 1997.

(25) *SMART 1000 CCD*; Bruker Analytical X-ray Systems: Madison, WI, 1999.

(26) *SAINT-Plus*, version 6.02 or later; Bruker Analytical X-ray Systems: Madison, WI, 1999.

(27) Sheldrick, G. *SHELXS-86: Program for Crystal Structure Solution*; Institüt für Anorganische Chemie der Universität: Göttingen, Germany, 1986.

(28) Sheldrick, G. *SHELXL-97: Program for Crystal Structure Refinement*; Institüt für Anorganische Chemie der Universität: Göttingen, Germany, 1997.

Table 1. Crystallographic Data

	[(**Ni-1′**)$_3$(ZnCl)$_2$](BF$_4$)$_2$	[(**Ni-1′**)$_3$(Cu$_2$Br)]Br	[(**Ni-1′**)$_3$Ag$_2$](ClO$_4$)$_2$	[(**Ni-1′**)$_3$Pb](ClO$_4$)$_2$
formula	$C_{27}H_{54}B_2Cl_2F_8N_6Ni_3S_6Zn_2$·3MeOH	$C_{27}H_{54}Br_2Cu_2N_6Ni_3S_6$·5 CH_2Cl_2	$C_{27}H_{54}Ag_2Cl_2N_6Ni_3O_8S_6$·$CH_3CN$	$C_{27}H_{54}Cl_2N_6Ni_3O_8PbS_6$
cryst syst	triclinic	monoclinic	rhombohedral	triclinic
space group	$P\bar{1}$	$P2_1/c$	$R\bar{3}c$	$P\bar{1}$
unit cell				
a (Å)	11.715(2)	15.0126(10)	11.8666(4)	11.654(5)
b (Å)	13.992(3)	15.1206(11)	11.8666(4)	14.460(5)
c (Å)	17.510(4)	25.0679(17)	110.290(5)	14.901(5)
α (deg)	100.720(4)	90	90	113.382(5)
β (deg)	105.571(3)	102.971(4)	90	108.483(5)
γ (deg)	110.265(3)	90	120	100.432(5)
V (Å^3)	2467.0(8)	5545.2(7)	13449.9(9)	2045.6(13)
Z	2	4	12	2
GOF	1.024	1.051	1.073	1.023
R1, wR2 [$I > 2s(I)$]	0.0544, 0.1350	0.0438, 0.0953	0.0430, 0.1285	0.0561, 0.1067
R1, wR2 (all data)	0.0806, 0.1505	0.0682, 0.1055	0.0499, 0.1314	0.0832, 0.1110

for structure refinement, and SHELXTL-Plus, version 5.1 or later (Bruker),[29] for molecular graphics and preparation of material for publication. The structures were solved by direct methods. Anisotropic displacement parameters were determined for all nonhydrogen atoms. Hydrogen atoms were added at idealized positions and refined with fixed isotropic displacement parameters equal to 1.2 times the isotropic displacement parameters of the atoms to which they were attached.

Results and Discussion

While a veritable library of N_2S_2 ligands exists, those based on structurally reinforced diazacycles offer the advantage that the number of isomers in the N_2S_2Ni complexes formed from them is limited. We selected the bme-dach ligand, structure **D**, for the following studies. It is synthetically more accessible than the bme-daco ligand, and in comparative structural studies thus far only minor differences have been observed.[5,21] It should be noted that the qualitative studies of metal binding preferences of $Zn^{2+} < Ni^{2+} \ll Cu^{+}$ which were published were based on the (bme-daco)Ni, **Ni-1**, complex in CH_3CN solutions.[11] Under similar conditions in CH_3CN solution, the same order of preference was found for the metallothiolate ligand, (bme-dach)Ni, **Ni-1′**. Shown in Figure 2 are the results of metal ion displacements in MeOH which largely mirror those in acetonitrile. Nevertheless, as indicated by the equilibrium arrows, nickel shows only a slight advantage over zinc; both the (**Ni-1′**)$_2$Ni^{2+} and the (**Ni-1′**)$_3$(ZnCl)$_2^{2+}$ clusters are observed in solutions containing mixtures of **Ni-1′**, Ni^{2+}, and Zn^{2+}.

In order to place the binding ability of **Ni-1′** in a broader context, binding constant measurements reported herein were carried out in aqueous media. Hence, the heterometallic clusters based on (bme-dach)Ni were prepared and characterized in order to identify the species formed during the aqueous titrations.

Preparation and X-ray Diffraction Structural Characterization of (Ni-1′)$_3$M$_2$ (M = Zn, Cu, Ag) and (Ni-1′)$_3$Pb Complexes. Simple combination of starting reagents, **Ni-1′**, and the exogenous metal source resulted in the four new polynuclear complexes for which crystallographic data are given in Table 1. Centrosymmetric space groups indicate

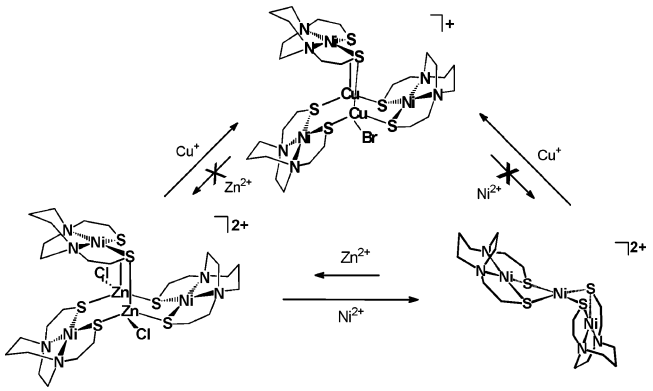

Figure 2. Qualitative metal ion displacements from **Ni-1′** in methanol.

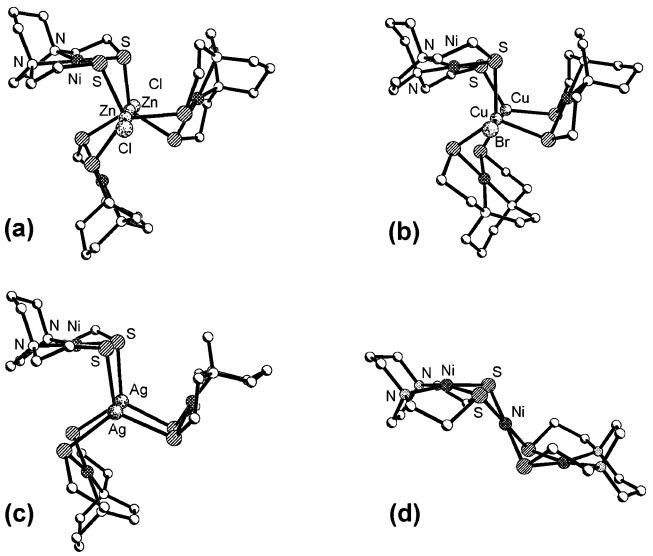

Figure 3. Ball-and-stick representations of the molecular structures of (a) [(**Ni-1′**)$_3$(ZnCl)$_2$]$^{2+}$, (b) [(**Ni-1′**)$_3$(Cu$_2$Br)]$^{+}$, (c) [(**Ni-1′**)$_3$Ag$_2$]$^{2+}$, and (d) [(**Ni-1′**)$_2$Ni]$^{2+}$ (ref 21) cations.

that crystallization resulted in racemic mixtures of the inherently chiral NiN_2S_2 derivatives. Figure 3 displays the molecular structures of the (**Ni-1′**)$_3$M$_2$ clusters, and selected distances and angles are given in Table 2. Full listings of all metric data are available in the Supporting Information. For comparison, metric data of the "free ligand", the **Ni-1′** complex, are also listed in Table 2. There are no significant differences between free **Ni-1′** and the **Ni-1′** which is engaged as a metallothiolate ligand in a bidentate, bridging arrange-

(29) *SHELXTL*, version 5.1 or later; Bruker Analytical X-ray Systems: Madison, WI, 1998.

Table 2. Selected Average Bond Distances and Angles and Averaged Uncertainties of (**Ni-1′**)$_3M_2$ Complexes Including **Ni-1′** for Comparison

	[(**Ni-1′**)$_3$(ZnCl)$_2$](BF$_4$)$_2$ *[(Ni-1)$_3$(ZnCl)$_2$](BF$_4$)$_2$*	[(**Ni-1′**)$_3$(Cu$_2$Br)](Br)	[(**Ni-1′**)$_3$Ag$_2$](ClO$_4$)$_2$	**Ni-1′**
M···M	4.28(1) *4.35(1)*	3.37(1)	3.00(1)	
M−S$_{avg}$	2.357(2) *2.355(5)*	2.355(2) Cu(1), 2.251(2) Cu(2)	2.515(2)	
M−X$_{avg}$	2.256(1) *2.269(8)*	2.633(1)		
Ni−S$_{avg}$	2.168(2) *2.186(5)*	2.169(2)	2.170(2)	2.164(1)
Ni−N$_{avg}$	1.917(5) *2.01(1)*	1.927(1)	1.932(5)	1.940(4)
M above S$_3$ plane$_{avg}$	0.630 *0.658*	0.229 Cu(1), 0.533 Cu(2)	0.2072 Ag(1), 0.0147 Ag(2)	
N−Ni−N$_{avg}$	83.0(2) *90.0(6)*	82.8(2)	82.8(2)	82.5(2)
S−Ni−S$_{avg}$	95.3(1) *88.1(2)*	95.0(1)	94.80(7)	94.4(1)
S−M−S$_{avg}$	113.0(1) *112*	115.0(1) Cu(1), 119.0(1) Cu(2)	119.997(1)	
S−M−X$_{avg}$	105.5(1) *106*	103.1(1)		

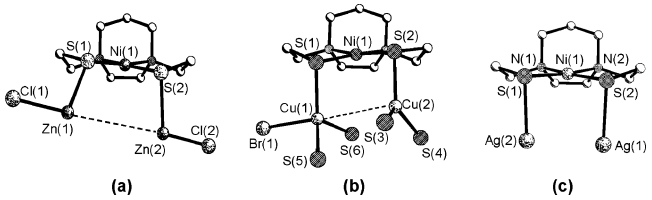

Figure 4. Comparison of the **Ni-1′** unit as a bidentate bridging ligand to the two central core metal ions of (a) [(**Ni-1′**)$_3$(ZnCl)$_2$]$^{2+}$, (b) [(**Ni-1′**)$_3$-(Cu$_2$Br)] Br, and (c) [(**Ni-1′**)$_3$Ag$_2$](ClO$_4$)$_2$.

ment leading to the pinwheel type structures. The structural forms and the metric data comparisons between the free and complexed NiN_2S_2 ligand of the (**Ni-1′**)$_3$(ZnCl)$_2^{2+}$ and the previously published (**Ni-1**)$_3$(ZnCl)$_2^{2+}$ clusters are largely the same.[30]

As seen in Figure 3a−c, the axes of the Ni_3M_2 pinwheels are $Ag^I\cdots Ag^I$, $BrCu^I\cdots Cu^I$, and $ClZn^{II}\cdots Zn^{II}Cl$ with M···M distances increasing in order 3.00(1), 3.37(1), and 4.28(1) Å, respectively. These differences highlight the ability of the N_2S_2Ni ligand to accommodate the trigonal planar preference of S_3Ag^I and also the tetrahedral preference of Zn^{II} in S_3ZnCl coordination. The latter places the zinc ions over 0.6 Å away from the best S_3 plane generated by the three bidentate-bridging **Ni-1′** units. The Cu···Cu distances are intermediate as one copper is 3-coordinate trigonal planar and the second is 4-coordinate tetrahedral. Another view of the M···M axes and the **Ni-1′** bridge is given in Figure 4. These drawings and the data in Table 3 emphasize the torsion angles defined by S−M···M−S which are significant in the **Ni-1′** derivatives. In contrast, the **Ni-1** version of the Ni_3Zn_2 pinwheel finds eclipsed S−Zn···Zn−S bonds, strictly planar Zn_2S_2 units, a linear Cl−Zn···Zn−Cl axis, and overall C_{3h} symmetry;[30] the **Ni-1′** analogue is of C_3 symmetry. Figure 3d is the slant chair structure of (**Ni-1′**)$_2$Ni^{2+}.[21]

The [(**Ni-1′**)$_3$Ag$_2$][ClO$_4$]$_2$ compound crystallized in a rhombohedral crystal system in which a 3-fold axis through the silvers generates the two remaining square planar N_2S_2Ni units, requiring ∠S−Ag−S ≡ 120.0°. Interestingly, Ag(1) is displaced out of its S_3 plane by 0.207 Å whereas Ag(2)S_3 is almost coplanar, with a Ag(2) displacement of 0.0147 Å. The hinge angle between the N_2S_2Ni and the S_2Ag_2 planes is 82.9(1)°. The sulfur−silver bond vectors are largely eclipsed with uniform S−Ag···Ag−S torsion angles of 4.0°.

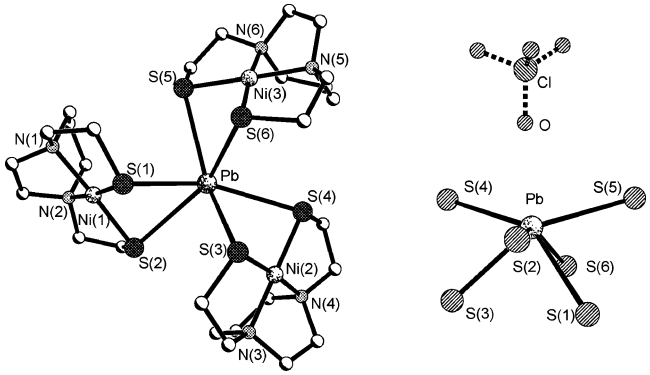

Figure 5. Ball-and-stick representation of the molecular structure of the [(**Ni-1′**)$_3$Pb]$^{2+}$ cation including an alternate view showing one perchlorate anion. Selected atoms were removed to better illustrate an "open" site indicating the stereochemically active lone pair of electrons. Selected averaged distances (Å) and angles (deg) with averaged uncertainties: Pb−S, 3.000(3); Ni−S, 2.136(4); Ni−N, 1.922(11); Pb···Ni, 3.49; S−Pb−S, 62.1; S−Ni−S, 93.00(15); N−Ni−N, 83.0(5).

The molecular structure shown in Figure 5 is of the product resulting from the reaction of **Ni-1′** with lead(II) perchlorate in CH_3CN, [(**Ni-1′**)$_3$Pb](ClO$_4$)$_2$; selected distances and angles are given in the figure caption. The three N_2S_2Ni units are bidentate chelating ligands to a hexacoordinate lead in pseudotrigonal antiprism coordination geometry. This presents an open face presumably mandated by the stereochemically active lone pair of Pb^{2+}.[31] The Pb−S distances opposite the "empty" coordination site range from 2.870(4) to 2.920(3) Å, and those near the stereochemically active lone pair range from 3.166(3) to 3.072(3) Å. These significant differences are consistent with the "hemidirected" terminology adopted to describe the irregular coordination geometry of Pb^{2+} complexes.[31] One of the perchlorate anions is positioned above the void in which the lone pair resides with a Pb···O

(30) Tuntulani, T.; Reibenspies, J. H.; Farmer, P. J.; Darensbourg, M. Y. *Inorg. Chem.* **1992**, *31*, 3497−3499.

Table 3. Torsion Angles, S−M···M−S, of (**Ni-1′**)$_3$M$_2$ Pinwheel Complexes

torsion angle (deg)	[(**Ni-1′**)$_3$(ZnCl)$_2$]-(ClO$_4$)$_2$	[(**Ni-1′**)$_3$(Cu$_2$-Br)](Br)	[(**Ni-1′**)$_3$Ag$_2$]-(ClO$_4$)$_2$
S(1)−M(1)−M(2)−S(2)	23.6	17.5	4.0
S(3)−M(1)−M(2)−S(4)	20.8	28.1	4.0
S(5)−M(1)−M(2)−S(6)	34.4	23.1	4.0

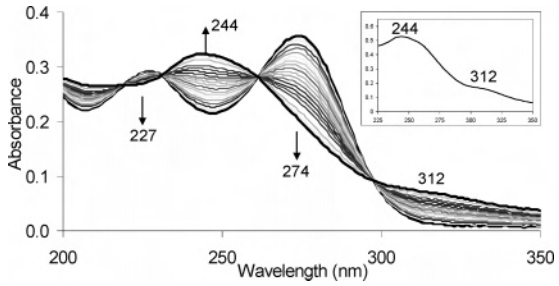

Figure 6. UV−vis spectral monitor of **Ni-1′** titrated with 20 μL additions of 0.1 M Cu$^+$. Inset spectrum is of the [(**Ni-1′**)$_3$Cu$_2$Br](Br) dissolved in water.

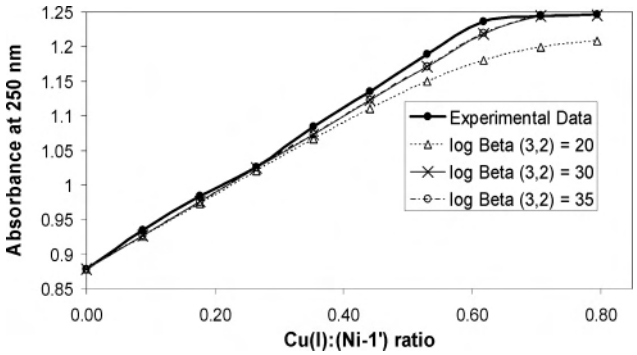

Figure 7. Experimental and calculated titration plots with varying values of log $\beta_{3,2}$ (see text) of the absorbance at 250 nm for **Ni-1′** titrated with Cu$^+$ versus the ratio of metal to ligand.

distance of 2.78(1) Å which is significantly longer than the average Pb−O bond distances in holodirected Pb(II) complexes, 2.53(15) Å.[31]

An interesting comparison of this structure is to be made with that of a complex of analogous composition, [(N$_2$S$_2$-Ni)$_3$Fe](ClO$_4$)$_2$ (N$_2$S$_2$Ni = *N*′,*N*′-dimethyl-*N*′,*N*′-bis(2-mercaptoethyl)-1,3-propanediamine).[32] The molecular structure contains a five-coordinate iron in which two of the N$_2$S$_2$Ni units bind in bidentate fashion and one in monodentate fashion. The pentacoordination preference of Fe^{II} in S-donor environment derived from N$_2$S$_2$Ni complexes is consistent with other structures.[33]

Titration Data for Formation and Composition of (Ni-1′)$_x$M$_y$ Aggregates in Aqueous Solution. Titrations of aqueous solutions of **Ni-1′** with solutions of metal salts were monitored by UV−vis spectroscopy. The spectral features were compared to those of the well-characterized mixed metal aggregates dissolved in water and in acetonitrile. Metal ion sources were perchlorate salts of Ag^I, Ni^{II}, Pb^{II}, and Zn^{II} dissolved in water. In order to prevent the disproportionation of Cu^I in water, the [Cu(NCMe)$_4$]PF$_6$ salt dissolved in acetonitrile was used as copper source. The distinct changes in the spectra during the Cu^I/**Ni-1′** titration, vide infra, were taken as evidence that this approach provided an unadulterated source of Cu^I for the formation of a **(Ni-1′)**$_3$Cu$_2$ cluster without such complications.

Orange-yellow aqueous solutions of **Ni-1′** display characteristic charge transfer absorptions with λ_{max} = 274 and 227 nm. Because of greater extinction coefficients and for instrumental reasons, these bands were used to monitor changes rather than the d → d transitions in the 400−500 nm region. With each 20 μL addition of 1 × 10^{-3} M [Cu(NCMe)$_4$]PF$_6$, the maxima diminished as bands at 244 nm and ca. 312 nm grew in, Figure 6. Four isosbestic points were clearly discernible, and the final spectrum overlapped well with that of [(**Ni-1′**)$_3$Cu$_2$Br]Br dissolved in water, Figure 6 inset. Figure 7 shows a plot of the absorbance at 250 nm versus the ratio of [Cu$^+$] to [**Ni-1′**] in which the change in slope at a metal/ligand ratio of 0.67 is consistent with the formation of a 2:3 cluster complex. The spectral monitor of the assembly of the (**Ni-1′**)$_3$Cu$_2$ cluster shows no intermediates, and there were no further changes with additional Cu(I) past the [Cu$^+$]/[**Ni-1′**] ratio of 0.67. Due to the high stability of the [(**Ni-1′**)$_3$Cu$_2$]$^{2+}$ complex in solution, even at the high dilution used in this study, formation of the complex was effectively stoichiometric. The calculated titration plots and the lower limit of log $\beta_{2,3}$ determinations will be described below.

Shown in Figure 8a are the overall changes in the UV−vis absorption spectra that occur upon addition of aqueous AgClO$_4$ to **Ni-1′** in water up to a ratio of 1:1. From these titration spectra, it is evident that two species are formed. Figure 8b isolates the changes occurring in [Ag$^+$]/[**Ni-1′**] ratios of 0−0.67. Four isosbestic points are discernible as the 227 and 274 nm bands for **Ni-1′** decrease and bands at 216 and 240 nm and the broad trailing band >300 nm appear. The bands which grow in produce a spectrum identical to that of a bona fide sample of [(**Ni-1′**)$_3$Ag$_2$]$^{2+}$ dissolved in water.

Figure 8c displays the subsequent spectral changes occurring in the [Ag$^+$]/[**Ni-1′**] range 0.67−1.0. Five isosbestic points may be identified as major bands at 216 and >300 nm diminish and two at 238 and 274 nm grow in. The new bands are attributed to the formation of a 2:2 complex which was supported by mass spectral data measured in water-(80%)/methanol(20%): [(**Ni-1′**)$_2$Ag$_2$]$^{2+}$, 385 *m*/*z*, 70% of the base peak (100% intensity at *m*/*z* 523 assigned to [(**Ni-1′**)$_3$Ag$_2$]$^{2+}$). Attempts to isolate the 2:2 complex thus far have yielded mixtures of the 3:2 and 2:2 complexes, see Supporting Information.

Up to a [Ni^{2+}]/[**Ni-1′**] ratio of 2.5 only minor changes in the spectrum of **Ni-1′** were observed. There was no percep-

(31) (a) Shimoni-Livny, S.; Glusker, J. P.; Bock, C. W. *Inorg. Chem.* **1998**, *37*, 1853−1867. (b) Hancock, R. D.; Reibenspies, J. H.; Maumela, H. *Inorg. Chem.* **2004**, *43*, 2981−2987.
(32) Colpas, G. J.; Day, R. O.; Mahoney, M. J. *Inorg. Chem.* **1992**, *31*, 5053−5055.
(33) Mills, D. K.; Hsaio, Y. M.; Farmer, P. J.; Atnip, E. V.; Reibenspies, J. H.; Darensbourg, M. Y. *J. Am. Chem. Soc.* **1991**, *113*, 1421−1423.

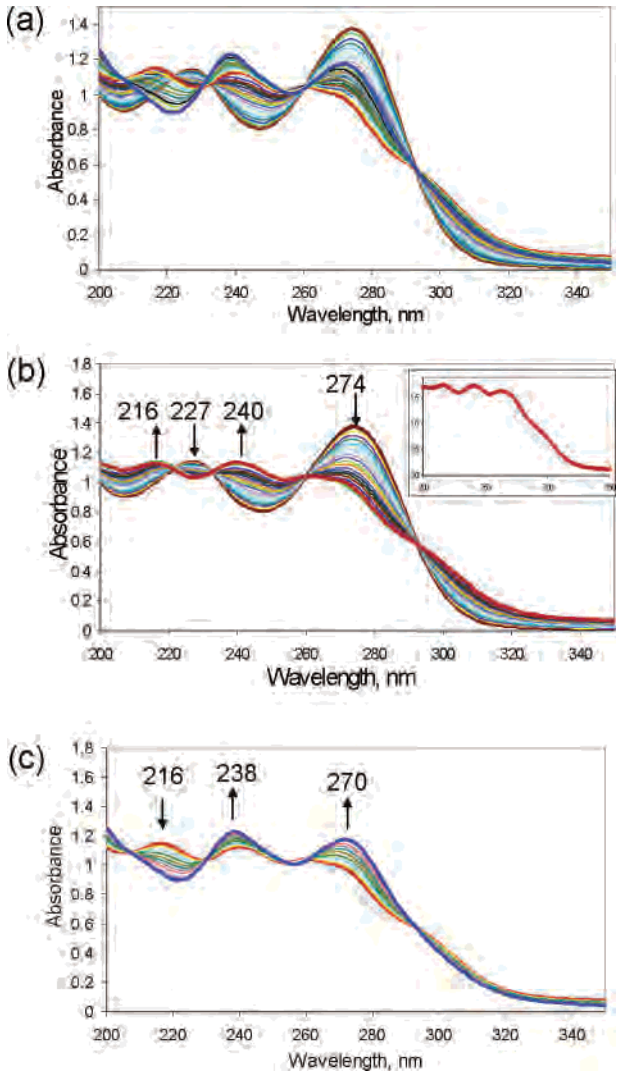

Figure 8. UV−vis spectra of aqueous **Ni-1′** titrated with 100 μL additions of 0.1 M $AgClO_4$: (a) range of Ag^+ equivalents added is 0−1.28, (b) formation of the 3:2 species with a range of Ag^+ equivalents of 0−0.67, and (c) formation of the 2:2 species with a range of Ag^+ equivalents of 0.67−1.28. Inset of part b is the spectrum of $[(\textbf{Ni-1}')_3Ag_2](ClO_4)_2$ dissolved in water.

tible change in color, and no build-up of the shoulder at 284 nm that might have indicated the formation of the trimetallic $[(\textbf{Ni-1}')_2Ni]^{2+}$ which is ubiquitous in nonaqueous solvents. Consistently, the aqueous spectrum of a bona fide sample of $[(\textbf{Ni-1}')_2Ni]^{2+}$ finds extensive dissociation of the trimetallic. The minor changes observed in the titration were subjected to plots of absorbance versus $[Ni^{2+}]/[\textbf{Ni-1}']$ ratio at specific wavelengths. As the observed curvature could not be attributed to simple dilution effects, it is interpreted in terms of the formation of small amounts of a 1:1 complex. The presence of such an adduct was supported by mass spectral data taken on 4:1 v/v H_2O/MeOH solutions containing **Ni-1′** to which 1.5 equiv of $Ni(OAc)_2{\cdot}6H_2O$ was added. An *m*/*z* signal at 393 (30%) was assigned to $[(\textbf{Ni-1}')Ni(OAc)]^+$.

The titration of **Ni-1′** with $Zn(ClO_4)_2$ also showed no color or spectral changes up to a 20-fold excess of zinc. With $Pb(ClO_4)_2$ where up to a 50-fold excess of $[Pb^{2+}]/[\textbf{Ni-1}']$ could be achieved, significant changes were seen over the course

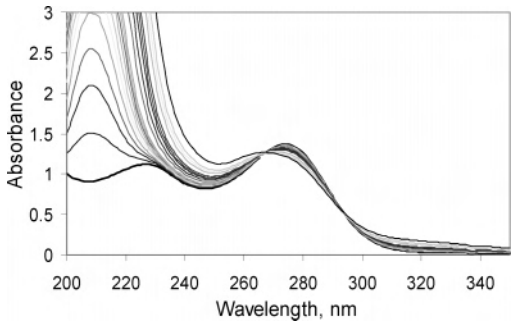

Figure 9. Electronic spectra of **Ni-1′** in water titrated with Pb^{2+}.

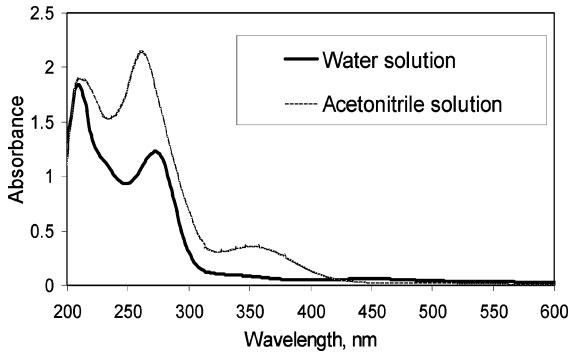

Figure 10. Comparative electronic spectra of aqueous and acetonitrile solutions of $[(\textbf{Ni-1}')_3Pb](ClO_4)_2$.

of titration, Figure 9. The **Ni-1′** band at 274 nm diminished, and an intense band at 210 nm grew in which is due to excess $Pb(ClO_4)_2$. The presence of two isosbestic points, at 265 and 294 nm, suggests only one product is formed. Furthermore, the absorption spectrum is similar to that of the isolated $[(\textbf{Ni-1}')_3Pb]^{2+}(ClO_4)_2$ salt dissolved in water; both are different from that observed in acetonitrile. That the cluster remained intact in the nonaqueous solvent was confirmed by mass spectral analysis (see Experimental Section and Supporting Information) which indicated the $[(\textbf{Ni-1}')_3Pb]^{2+}$ (519 *m*/*z*) as the most intense of the Pb/Ni species in CH_3CN. However, in water the most intense Pb-containing signal (145 *m*/*z*) corresponded to $[Pb(CH_3OH)(OH_2)]^{2+}$, and no (**Ni-1′**)/Pb adducts were detected.

The electronic spectra of $[(\textbf{Ni-1}')_3Pb]^{2+}$ in water versus acetonitrile are shown in Figure 10. The differences include an obvious band at 352 nm in the acetonitrile solution which is attributed to the Pb−S interaction; this band is barely visible if not absent in the aqueous solution. The aqueous solution spectrum, however, has a broad band at 450 nm which is characteristic of free **Ni-1′**. Other obvious differences exist in intensity ratios in the 200−300 nm region.

From the results in Figure 10, it is concluded that substantial dissociation of the $[(\textbf{Ni-1}')_3Pb]^{2+}$ complex occurs in water. Nevertheless, the isosbestic points observed in the spectral titrations argue for complexation between aqueous Pb^{2+} and **Ni-1′**. Therefore, for the purposes of computing formation constants, we have assumed a 1:1 composition for a Pb^{2+} to **Ni-1′** adduct in water.

Binding Constant Computations. In order to quantify the binding affinity of the N_2S_2Ni metallodithiolate ligand L, equilibrium constants for the capture of metal ions by **Ni-1′** were determined according to eqs 1−3, making use

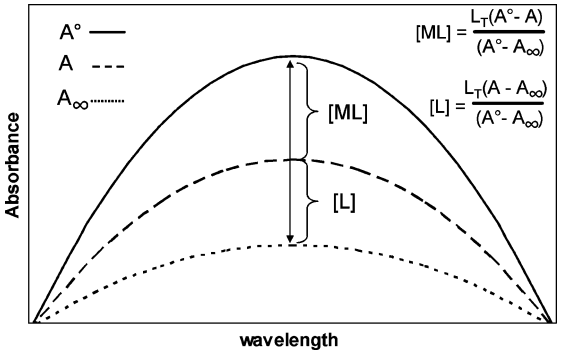

Figure 11. Illustration of the determination of concentrations of complex, ML = (**Ni-1′**)M^{2+}, and ligand, L = **Ni-1′**.

of multiple data points at a specific wavelength.

$$K = [ML]/([L][M]) \quad (1)$$

$$[M_T] = [M] + [ML] \quad (2)$$

$$K = [ML]/\{[L]([M_T] - [ML])\} \quad (3)$$

Figure 11 illustrates the definitions used to obtain values for the concentrations of [ML], the metal/ligand complex, and [L], the free N_2S_2Ni metallothiolate ligand. For the [(**Ni-1′**)Pb]$^{2+}$ complex, the amount of free metal ion [M] was approximated by [M] = [M_T] (total metal ion added) as large excesses of Pb^{2+} were required to reach A_∞. The computed K values averaged over 20−50 data points were further used to compute absorbance values in order to graphically compare the experimental with the computed absorbance decay or build-up. In this manner, the log K values for Ni^{2+}, Pb^{2+}, and Zn^{2+} were determined to be 2.2, 2.1, and 2.0, respectively.

$$A = \frac{K[M_T]A_\infty + A^0}{1 + K[M_T]} \quad (4)$$

Due to the complexity of the equations for the silver and copper titrations which form (**Ni-1′**)$_3M_2$ cluster species, a computer program was written that used multiple iterations to assess log $\beta_{3,2}$. Graphs were generated using various values for log $\beta_{3,2}$ to best fit the experimental curves. The experimental curve of the absorbance at 275 nm for the titration of Ag^+, Figure 12, shows the formation of the (**Ni-1′**)$_3M_2$ species and then conversion to another species. It also shows the computer-generated curves at various values of log $\beta_{3,2}$. The best fit curve for the formation of [(**Ni-1′**)$_3Ag_2$]$^{2+}$ converged on log $\beta_{3,2}$ = 26.

Attempts to match the absorbance at 250 nm for **Ni-1′** titrated with Cu^+ resulting in formation of [(**Ni-1′**)$_3Cu_2$]$^{2+}$ found that even the largest log $\beta_{3,2}$ values could not generate the experimental curve, Figure 7. All that can be said is that the log $\beta_{3,2}$ value is greater than 30. The formation constants determined in this study are listed in Table 4, together with log K_1 values for a thiolate, mercaptoethanol, and a thioether, thiodiethanol, for comparison with the same metal ions for which binding constants were determined.

Comments and Conclusions

Synthetic designs based on a view of the N_2S_2Ni complex as an innocent cis-dithiolate sulfur donor and a building block

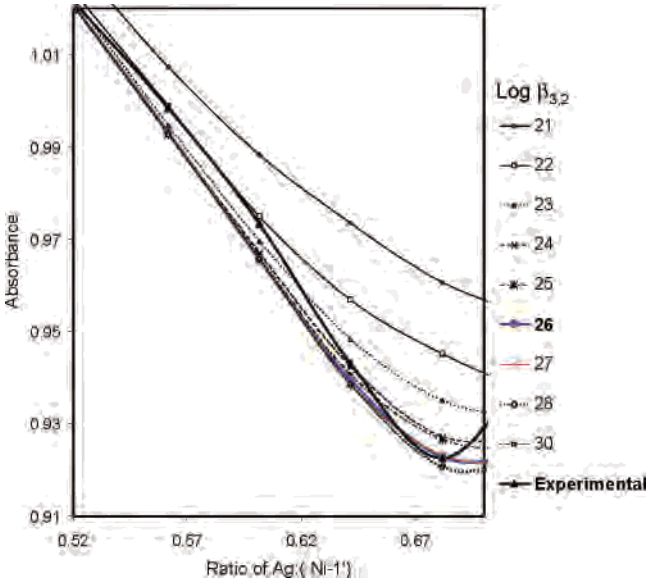

Figure 12. Experimental and calculated (varying log $\beta_{3,2}$) plots for the absorbance at 275 nm of **Ni-1′** titrated with Ag^+ versus the ratio of metal to ligand.

Table 4. Formation Constants (log $\beta(M_nL_m)$) for Metal Ion Complexes with L = [(bme-dach)Ni] Determined at 25 °C and Ionic Strength ~0 for Various Metal Ions, Compared with log K_1 Values for Mercaptoethanol (ref 1) as an Example of Mercapto Ligand, and Thiodiethanol as an Example of a Thioether

	Cu^+	Ag^+	Ni^{2+}	Pb^{2+}	Zn^{2+}
			log K_1		
L = mercaptoethanol	(16.7)[a]	13.7[a]	(3.2)[a]	6.6	(5.7)[a]
L = thiodiethanol	(3.6)[a]	3.53	−0.16	(0.4)[a]	−0.18
			log $\beta(M_nL_m)$		
L = [bme-dach)Ni]	>30	26	2.2	2.1	2.0
n, m in M_nL_m	2, 3	2, 3	1, 1	1, 1	1, 1

[a] Estimated as described in ref 34.

for heterometallic clusters have been vastly successful. With judicious use of steric hindrance to block extensive aggregation, dinuclear derivatives are appropriate to small molecule models of the acetyl CoA synthase enzyme active sites.[9,10] Without the steric blocks, the extent of polynucleation is indicative of the significant affinity that nickel thiolates have for other metals.[11,20−22,30] In particular, the fact that Cu(I) and Ag(I) were able to form self-assembled, bridged clusters of the (**Ni-1′**)$_3M_2$ type even at the low concentrations used in this study, and in aqueous media, shows the high affinity that these metal ions have for sulfur donors in general, specifically, for the sulfurs in the N_2S_2Ni metallothiolate ligands. Interestingly, although lead is typically considered sulfophilic, existing in nature primarily as the sulfide ore galena, water and methanol solvate interactions compete well with S-donors of N_2S_2Ni ligands for the coordination sphere of lead.

Classical metal ion titration studies have generated quantitative and comparative data for the binding ability of these nonclassical metallothiolate donor ligands. In the simple cases of 1:1 adducts as in (**Ni-1′**)Zn^{2+}, (**Ni-1′**)Ni^{2+}, and (**Ni-1′**)Pb^{2+}, direct comparison of log K_1 values with those of the mercaptoethanol thiolate and the thiodiethanol thioether find the order of S-donor strengths is RS^- > NiSR > R_2S.

For numerical comparison to the 1:1 adducts, there is, unfortunately, no direct way of determining log K_1 for Ag^+ or Cu^+ from the log $\beta_{3,2}$ values. We suggest a reasonable approximation follows from examination of ligand/metal systems where both the log K_1 and log $\beta_{3,2}$ values are known. Thus, one finds for thioglycolic acid ($HOOCCH_2S^-$) that log $K_1 \sim {}^1/_3$ of log $\beta_{3,2}$ for metal ions such as Ni(II) and Zn(II) which form $(O-S)_3Ni$ or $(O-S)_3Zn$ complexes.[35] Assuming a similar result for our cluster systems, the log K_1 for the (**Ni-1′**)$_3M_2$ formulations would be ca. 8 for Ag^+ and >10 for Cu^+.

Thus, in all cases explored in our studies, the binding ability of Ni−S−R for metal ions is intermediate between that of a free thiolate and a free thioether. There is a great specificity for copper and silver over nickel, zinc, and lead; however, the latter three have similar affinities for the N_2S_2-Ni metallothiolate ligand.

The similarities in the **Ni-1** and **Ni-1′** metallodithiolate ligands have been emphasized in this report. In fact, there are solvent-dependent, subtle differences in binding affinities of **Ni-1** and **Ni-1′** for Ni^{2+} vs Zn^{2+}. The difference in the S−Ni−S angles, 90° in **Ni-1**, and 95° in **Ni-1′**, may account for the binding preferences; the smaller bite angle of **Ni-1** more readily conforms to the square planar coordination geometry preference of Ni(II) and the formation of the "mononuclear" L_2Ni^{2+} complex. The solvent effect illustrates the balance of factors that engender cluster formation on the mixed metal compounds. The oxygen donors of water and methanol compete well with the sulfur donors of N_2S_2Ni for the divalent cations Ni(II), Zn(II), and Pb(II), while in acetonitrile the N_2S_2Ni ligation ties up all available binding sites.

With regard to the protein crystal structures of acetyl CoA synthase and the myriad of metals found by this technique in the active site, it should be noted that ongoing biochemical studies probe whether metal replacement processes occurred during the enzyme isolation process or an incorrect metal insertion occurred during cell growth.[14,17,38] At this point, the results are not definitive. While knowledge of specific mechanisms of nickel uptake, excluding other metal ions such as copper, is in an early stage of discovery, it is known that complex assemblies of accessory proteins are required for metal trafficking.[36,37,39] Our fundamental solution studies establish thermodynamic preferences and, thereby, a simple fact: *When stripped of the biochemical machinery which controls intracellular metal ion concentration, the thiolate sulfurs of exposed N_2S_2Ni sites could scavenge and bind available copper(I) ions at a minimum of 6−8 orders of magnitude greater than nickel or zinc ions.* Such large binding constants as determined here, as well as the qualitative studies which established the ability of Cu(I) to replace Zn(II) and Ni(II) when bound to N_2S_2Ni,[11] should alert biochemists of the potential ambiguities from even trace copper at impurity levels in liquid media containing the isolated protein. It should be noted that the oxidation state of copper, Cu(II) (the likely form in buffers) or Cu(I), is irrelevant as Cu(II) is readily reduced to Cu(I) in the presence of thiols[40] as well as the N_2S_2Ni complexes (see Supporting Information). In the latter case, the same pentanuclear Ni_3Cu_2 clusters are obtained with both Cu(II) and Cu(I) sources. Given the plentitude of structures that show multiple copper−sulfur interactions, one might also expect more than one copper to bind to cellular-compromised N_2S_2Ni as well as FeS sites.[14,17,22]

Acknowledgment. The authors thank the NSF (Grant CHE 01-11131 to R.D.H. and CHE 01-11629 to M.Y.D.), the R.A. Welch Foundation (M.Y.D.), and the University of North Carolina at Wilmington (R.D.H.) for support of this work. The X-ray diffractometers and crystallographic computing systems in the X-ray Diffraction Laboratory at the Department of Chemistry, Texas A&M University, were purchased from funds provided by the National Science Foundation.

Note Added after ASAP Publication: Some notation was incorrect in Figure 11 in the version of this paper published on the Web January 5, 2005. The version published on the Web January 12, 2005, has been corrected.

Supporting Information Available: Determination of formation constants. Complete details (CIF format) of the X-ray diffraction studies for compounds {[**Ni-1′**]$_3$(ZnCl)$_2$}(BF$_4$)$_2$, {[**Ni-1′**]$_3$-(Cu$_2$Br)}Br, {[**Ni-1′**]$_3$Ag$_2$}(ClO$_4$)$_2$, and {**[Ni-1′**]$_3$Pb$_2$}(ClO$_4$)$_2$ with ORTEP plots. Figures for mass spectral isotopic patterns for {**[Ni-1′**]$_3$(Cu$_2$Br)}Br, {[**Ni-1′**]$_3$Ag$_2$}(ClO$_4$)$_2$, and {**[Ni-1′**]$_3$Pb$_2$}(ClO$_4$)$_2$ species. This material is available free of charge via the Internet at http://pubs.acs.org.

IC0489701

(34) Martell, A. E.; Hancock, R. D. *Metal Complexes in Aqueous Solutions*; Plenum Press: New York, 1996; p 48.
(35) Anderegg, G.; Malik, S. C. *Helv. Chim. Acta* **1970**, *53*, 577.
(36) Kuchar, J.; Hausinger, R. P. *Chem. Rev.* **2004**, *104*, 509−525.
(37) Mulrooney, S. B.; Hausinger, R. P. *FEMS Microbiol. Rev.* **2003**, *27*, 239−261.
(38) Tan, X.; Bramlett, M. R.; Lindahl, P. A. *J. Am. Chem. Soc.* **2004**, *126*, 5954−5955.
(39) Pena, M. M. O.; Lee, J.; Thiele, D. J. *J. Nutr*. **1999**, *129* (7), 1251−1260.
(40) Gilbert, B. C.; Silvester, S. Walton, P. H. *J. Chem. Soc., Perkin Trans. 2* **1999**, 1115−1121.